Variational *Ansatz* for the Ground State of the Quantum Sherrington-Kirkpatrick Model

Paul M. Schindler,[1,2,*] Tommaso Guaita,[2,3,4,†] Tao Shi,[5,6] Eugene Demler,[7] and J. Ignacio Cirac[2,3]
[1]*Max-Planck-Institut für Physik komplexer Systeme, Nöthnitzer Straße 38, 01187 Dresden, Germany*
[2]*Max-Planck-Institut für Quantenoptik, Hans-Kopfermann-Straße 1, 85748 Garching, Germany*
[3]*Munich Center for Quantum Science and Technology, Schellingstraße 4, 80799 München, Germany*
[4]*Dahlem Center for Complex Quantum Systems, Freie Universität Berlin, Arnimallee 14, 14195 Berlin, Germany*
[5]*CAS Key Laboratory of Theoretical Physics, Institute of Theoretical Physics, Chinese Academy of Sciences, Beijing 100190, China*
[6]*CAS Center for Excellence in Topological Quantum Computation, University of Chinese Academy of Sciences, Beijing 100049, China*
[7]*Institute for Theoretical Physics, ETH Zurich, Wolfgang-Pauli-Straße 27, 8093 Zurich, Switzerland*

(Received 2 May 2022; revised 13 September 2022; accepted 31 October 2022; published 21 November 2022)

We present an *Ansatz* for the ground states of the quantum Sherrington-Kirkpatrick model, a paradigmatic model for quantum spin glasses. Our *Ansatz*, based on the concept of generalized coherent states, very well captures the fundamental aspects of the model, including the ground state energy and the position of the spin glass phase transition. It further enables us to study some previously unexplored features, such as the nonvanishing longitudinal field regime and the entanglement structure of the ground states. We find that the ground state entanglement can be captured by a simple ensemble of weighted graph states with normally distributed phase gates, leading to a volume law entanglement, contrasting with predictions based on entanglement monogamy.

DOI: 10.1103/PhysRevLett.129.220401

Introduction.—Spin glasses are an important paradigm in statistical physics. Besides their relevance in describing disordered classical magnets [1,2], it was shown that optimization tasks, such as the traveling salesman problem, can be mapped to solving for the ground states of spin glass systems [1,3,4]. Classical spin glasses can be promoted to quantum models by introducing a transverse field. The resulting quantum spin glasses form by themselves an important playground to study the interplay of disorder and frustration with quantum effects [5]. Moreover, there is evidence that the quantumness can be exploited to shortcut optimization tasks, for instance, through quantum annealing [6–10].

The textbook example of a quantum spin glass model is the quantum Sherrington-Kirkpatrick (QSK) model, a generalization of the classical Sherrington-Kirkpatrick (SK) model [11,12]. The QSK model has been studied extensively in the literature both analytically [12–18] and numerically [19–30]. While the famous Parisi solution [31,32] provides a full solution to the classical SK model, many open questions remain for the quantum SK model. Since the QSK model is an all-to-all coupled model one might assume that a mean-field product state *Ansatz* well describes the ground state. However, this *Ansatz* predicts a quantum phase transition from a quantum spin glass phase to a paramagnetic phase at a critical transverse field $g_C \approx 2J$ [26]. Field theory approaches [15,16,18] using the replica method suggest instead a phase transition at $g_C \approx 1.5J$. Numerical calculations at small system sizes [23,24,33] or obtained at finite temperature [19,20,24,29,34] confirm the latter [35]. So far no good *Ansätze* have been found which can describe the zero temperature regime for large system sizes, preventing the study of further properties of the ground state, such as entanglement.

Here, we consider a variational family, motivated by the concept of generalized group-theoretic coherent states [36], which extends the product state *Ansatz* introducing a richer entanglement structure. The special structure of these states allows us to introduce nontrivial quantum correlations while preserving the ability to efficiently compute variational ground states up to large system sizes of $N = 200$ spins. We additionally develop a method to study the entanglement structure of the ground states. Our results show a volume law of entanglement, which indicates that entanglement monogamy does not provide a scaling constraint despite the fact that the QSK model involves all-to-all spin interactions. Furthermore, this entanglement structure is also identified within a set of states that have been introduced in the quantum information context, namely

weighted graph states [37] with normally distributed random phase gates.

Model.—Concretely, the QSK model corresponds to a mixed field Ising model with all-to-all couplings between the N spins and quenched disorder in the couplings and longitudinal field,

$$H_{\mathrm{QSK}} = -\frac{1}{2}\sum_{n,m=1}^{N} J_{nm}\sigma_n^z\sigma_m^z - g\sum_{n=1}^{N}\sigma_n^x - \sum_{n=1}^{N} h_n\sigma_n^z, \quad (1)$$

where σ_n^k is the kth Pauli matrix acting on the nth spin. The longitudinal field h_n and the couplings J_{nm} are independently normally distributed numbers with zero mean and variance $\overline{h_n^2} = h^2$ and $\overline{J_{nm}^2} = J/N$, respectively. Here and in the following we use the convention that an overbar indicates disorder average, and we will mostly concentrate on the case $h = 0$.

Variational Ansatz.—Our variational *Ansatz* was first introduced in Refs. [38,39]. It generalizes the *Ansatz* of atomic coherent states (CS) [40],

$$|\phi(\boldsymbol{x})\rangle = \mathcal{U}(\boldsymbol{x})|\uparrow,\ldots,\uparrow\rangle, \quad (2)$$

where $\sigma^z|\uparrow\rangle = +|\uparrow\rangle$ and $\mathcal{U}(\boldsymbol{x}) = \exp(-i\sum_{n,k} x_n^k\sigma_n^k)$ rotates each of the N spins individually on the Bloch sphere. The CS *Ansatz* is parametrized by $x_n^k \in \mathbb{R}$ and corresponds to the set of normalized product states.

A generalization procedure [36] leads to generalized atomic coherent states (GCS),

$$|\Psi(\boldsymbol{x},\boldsymbol{y},\boldsymbol{M})\rangle = \mathcal{U}(\boldsymbol{y})\mathcal{V}(\boldsymbol{M})|\phi(\boldsymbol{x})\rangle, \quad (3)$$

where x_n^k, y_n^k, and M_{nm} $(n < m)$ are the variational parameters. $\mathcal{U}$ and $|\phi\rangle$ are defined as in Eq. (2) and the entangling unitary $\mathcal{V}(\boldsymbol{M})$ is given by

$$\mathcal{V}(\boldsymbol{M}) = \exp\left(-\frac{i}{4}\sum_{n<m} M_{nm}\sigma_n^z\sigma_m^z\right), \quad (4)$$

for any real symmetric matrix $\boldsymbol{M}$.

The entangling unitaries $\mathcal{V}(\boldsymbol{M})$ contain two-spin terms which give the states (3) a nontrivial correlation structure. Nonetheless, when computing expectation values of Pauli operators we have $\mathcal{V}(\boldsymbol{M})^\dagger\sigma_n^\pm\mathcal{V}(\boldsymbol{M}) = \sigma_n^\pm\exp(\pm i/4\sum_m M_{nm}\sigma_m^z)$; that is, the two-spin terms cancel and we are left with just products of single-spin operators [36,41]. This crucial property allows us to find analytical expressions for the energy and the gradient of the energy with respect to the variational parameters [42]. Thanks to this, we can efficiently obtain the variational ground states of individual Hamiltonian realizations for large system sizes of up to $N = 200$ spins through a natural gradient descent algorithm [43].

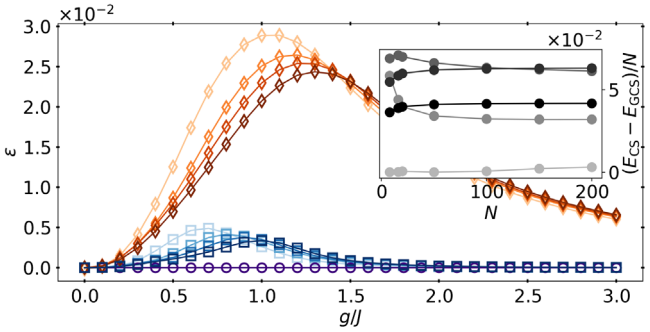

FIG. 1. Average error in energy density $\epsilon = \overline{\Delta E}/\overline{W}$ as a function of the transverse field for different methods (CS in orange, GCS in blue, and ED in purple) and system sizes $N = 8$, 12, 16, 22 (light to dark). ΔE is the difference between the variational energy and the exact ground state energy, W is the difference between the highest and lowest energies in the exact spectrum. Inset: difference between CS and GCS energies per site $(E_{\mathrm{CS}} - E_{\mathrm{GCS}})/N$ as a function of the system size N for different values $g/J = 0.1$, 1.0, 1.5, 2.0, 3.0 (light to dark). All data are for $h = 0$ and averaged over $n_{\mathrm{samples}} = 1000$ disorder realizations.

To demonstrate the expressivity of the GCS *Ansatz*, we first consider the approximate ground state energy. For small system sizes we can compare the variational energies with numerically exact results, obtained via a Lanczos exact diagonalization (ED) method [44]; see Fig. 1. We find good quantitative agreement of the variational energy with the exact ground state energy over a broad range of transverse and longitudinal field values. In particular, a notable improvement of the GCS *Ansatz* upon the CS *Ansatz* becomes visible. The method performs worst in a region with $0.5J < g < 1.5J$. For the assessed system sizes, the point of maximal error moves with growing N toward the expected critical point $g_C \approx 1.5J$, while the maximal error value decreases [45]. This agreement is not limited to the energy but can also be seen for other observables of interest [46].

For larger systems it is no longer possible to compare to an exact solution. However, we observe an extensive improvement in energy upon the CS *Ansatz*, suggesting that the GCS *Ansatz* gives a nonvanishing improvement even in the thermodynamic limit; see inset of Fig. 1.

Quantum phase transition.—Our variational *Ansatz* also allows us to study the quantum phase transition on the $h = 0$ line of the model's parameter space. For this we consider the spin glass susceptibility $\chi_{\mathrm{sg}} = N^{-1}\sum_{n,m}\overline{\langle\sigma_n^z\sigma_m^z\rangle^2}$. Indeed, the susceptibility per site χ_{sg}/N, which is independent of the system size in the thermodynamic limit, vanishes in the paramagnetic phase (large g) and is finite in the spin glass phase (small g) [1,23,27,47,48]. For small system sizes we find good quantitative agreement of the variational value of the susceptibility with numerically exact (ED) results; see left-hand panel of Fig. 2. More importantly, the variational *Ansatz* enables us to study the system at much larger sizes;

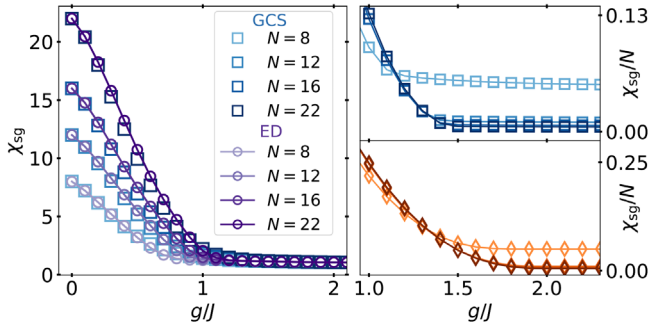

FIG. 2. Left: spin glass susceptibility χ_{sg} as a function of the transverse field g for ED (purple circles) and GCS (blue squares). Right: spin glass susceptibility per site χ_{sg}/N for GCS (top, blue) and CS (bottom, orange) and system sizes $N = 20$, 100, 200 (from light to dark). All data are for $h = 0$ and averaged over $n_{\mathrm{samples}} = 1000$ disorder realizations.

see right-hand panels of Fig. 2. For $N \geq 100$ finite size effects are almost absent, allowing us to read off the critical field value directly. Both variational *Ansätze* clearly indicate the existence of a phase transition. However, in agreement with the literature [26], the CS underestimate the quantum fluctuations showing a phase transition at roughly $g_C \approx 2J$. In contrast, the GCS capture the true critical point at $g_C \approx 1.5J$. Thus, the additional entanglement structure introduced in the GCS not only leads to an improvement in energy but also seems crucial in capturing the physics of the QSK model in the thermodynamic limit. This agreement with established results further indicates that the variational states remain a good approximation of the ground states in the large N limit.

Entanglement structure of the ground state.—The findings above suggest that the GCS *Ansatz* describes the ground state of the QSK model very well for all system sizes up to the thermodynamic limit. Having such an explicit expression for the ground state wave function allows us to study in detail its entanglement properties. Before looking into the numerical results, we will consider some hypotheses about the expected entanglement behavior.

First, let us try to understand the role of the additional two-spin entangling gates contained in $\mathcal{V}(\boldsymbol{M})$ by taking a closer look at the matrix elements M_{nm}. Considering the probability distribution $p(M_{nm})$ over many disorder realizations, we observe that it resembles a Gaussian distribution with zero mean and variance scaling as $1/N$. In addition, we find that the mean level spacing ratio averaged over many realizations yields $\overline{\langle r \rangle} \approx 0.53$ roughly independent of the transverse field value $g > 0$ and system size N, which is in agreement with the result of the Gaussian orthogonal ensemble (GOE) [49].

This implies that most two-spin entangling gates approach the identity as $N \to \infty$. This may seem compatible with the naive hypothesis that, due to the mean-field nature of the model, product states should well describe the ground state, at least in the thermodynamic limit. This assumption would predict the entanglement entropy between any two subsystems going to zero as $N \to \infty$.

Note, however, that the number of entangling gates acting on each individual spin diverges in this limit, suggesting that a nontrivial entanglement structure is still possible. Indeed, let us consider a subsystem A composed of the first L spins. We quantify the entanglement between these L spins and the rest of the system by computing the second Rényi entropy $S_2(L)$ of the subsystem's reduced density matrix. Given the all-to-all connectivity of our *Ansatz*, there exist $L(N-L)$ two-spin entangling gates acting between spins in A and in its complement A^c. Each of these gates individually generates a two-spin state with an average entanglement entropy proportional to $\overline{M_{nm}^2} \sim 1/N$. The cancellation of these two scalings could suggest a second hypothesis, i.e., that the entanglement entropy between A and A^c is proportional to L in the thermodynamic limit $N \to \infty$. This expectation can also be made more rigorous with an argument based on the central limit theorem [42].

As a third alternative, we may compare the model to a related but analytically solvable model, namely a model with all-to-all interactions and invariant under spin permutations. Note that in our case, due to the disordered nature of the QSK model, individual realizations of the couplings J_{nm} and h_n are not permutationally invariant. However, invariance is present upon disorder averaging, so the permutationally invariant case may still provide a useful comparison. In such case the ground state $|\Psi\rangle$ must possess a Schmidt decomposition,

$$|\Psi\rangle = \sum_k \lambda_k |\varphi_k\rangle |\eta_k\rangle, \tag{5}$$

where $|\varphi_k\rangle$ and $|\eta_k\rangle$ are orthonormal states of A and A^c, respectively. Because of the symmetry, the states $|\varphi_k\rangle$ must in particular belong to the subspace of permutationally invariant states of A. Such subspace has dimension $L+1$, so there can be at most $L+1$ terms in the sum (5). It follows that the entanglement entropy of A is bounded by $S_2(L) \leq \log(1+L)$. This scaling of the entanglement can be viewed as a consequence of entanglement monogamy [50,51].

We would now like to compare our results with these hypotheses. To this end, we have developed an efficient method to numerically compute $S_2(L)$ for the states (3), reducing the problem to the one of estimating averages for a classical sampling problem [42]. The results, see top panel of Fig. 3, are well fitted by the empirical functional form:

$$\overline{S_2(L;N)} = A(N) \log\left[1 + \frac{B(N)}{\pi} \sin\left(\frac{\pi L}{N}\right)\right]. \tag{6}$$

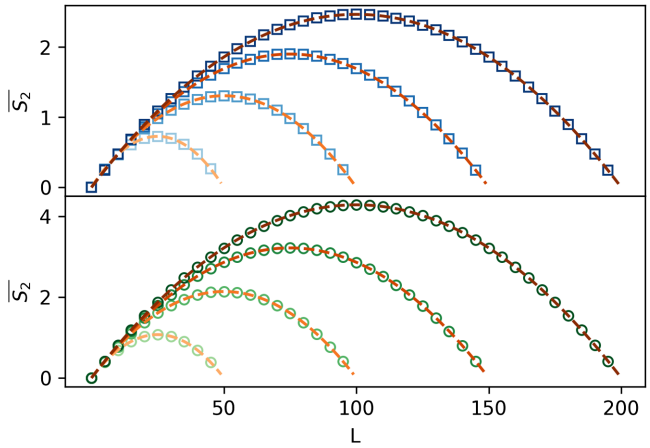

FIG. 3. Average Rényi-2 entanglement entropy as a function of the subsystem size L for the QSK ground state at $g = 1J$, $h = 0$ (top panel in blue) and for an ensemble of weighted graph states (7) (bottom panel in green). Data are plotted for total system sizes $N = 50$, 100, 150, 200 (from light to dark markers). In all cases, including ground state data for other values of the fields g and h, the entropy is well fitted by the function (6) (orange dashed lines).

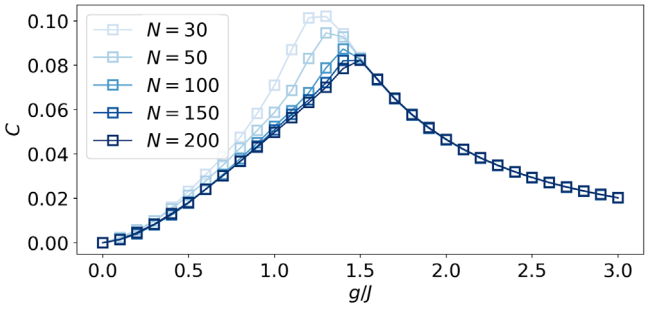

FIG. 4. Coefficient $C(N)$ extrapolated from the Rényi entanglement entropy fit as a function of the transverse field g at $h = 0$ for different system sizes (different shades of blue).

Note that, in the large N limit, this functional form may alternatively represent a $\overline{S_2(L)} \sim L$ scaling, a $\overline{S_2(L)} \to 0$ scaling, or a $\overline{S_2(L)} \sim \log L$ scaling of the entropy, depending on the behavior of the fit parameters $A(N)$ and $B(N)$.

In the range of system sizes that we were able to explore ($N \leq 200$), we observe that the parameter $B(N)$ converges to a finite constant as $N \to \infty$. Similarly, the product $C(N) \equiv A(N)B(N)/N$ also converges to a constant C. This suggests the asymptotic behavior $\overline{S_2(L;N)} = CL + \mathcal{O}(1/N)$ in the thermodynamic limit. In other words, we observe an entanglement scaling proportional to the volume L of the considered subsystem, that is larger than the one both of a product state description and of a permutationally invariant model.

Finally, we point out that the entanglement structure of the ground states appears to encode very clearly the phase transition of the model. More specifically, if we compute the fit coefficient $C(N)$ defined above as a function of the transverse field g at $h = 0$, we will see that this function develops, in the thermodynamic limit, a discontinuity in its derivative at the critical value $g_C \approx 1.5J$, as shown in Fig. 4.

Comparison to random weighted graph states.—The form of the matrix $\boldsymbol{M}$, which appears to be distributed according to a GOE, suggests that the entanglement structure of the QSK ground states is encoded in a simple way in $\mathcal{V}(\boldsymbol{M})$. To see this better, consider the set of states parametrized as

$$|\Psi(\boldsymbol{M})\rangle = \mathcal{V}(\boldsymbol{M})|+,\cdots,+\rangle, \tag{7}$$

where $|+\rangle = (1/\sqrt{2})(|\uparrow\rangle + |\downarrow\rangle)$. These are a subset of the full variational class (3) and, in the context of quantum information theory, are referred to as *weighted graph states* [37]. Let us then consider a random ensemble of such states constructed by drawing the matrix $\boldsymbol{M}$ from a GOE with variance $\overline{M_{nm}^2} = 1/N$.

We can compute the average subsystem entanglement entropy $\overline{S_2(L)}$ for this ensemble of states, similarly to what we did for the ground states. We find that this entropy is fitted by the same functional form (6), see bottom panel of Fig. 3, and that the fit parameters $A(N)$ and $B(N)$ obey the same large N scalings as in the ground state case. It is also possible to show analytically that the entanglement of these states must scale according to a volume law, as confirmed by these fits [42].

We conclude that the simple form (7), where $\boldsymbol{M}$ is sampled from a GOE, exhibits the key entanglement features of the QSK ground states. It can be taken as a minimal example of this entanglement structure.

Let us stress, however, that the actual ground states still contain more information than the states (7). The state $|\boldsymbol{\phi}(\boldsymbol{x})\rangle$ appearing in the variational *Ansatz* (3) is in general not equal to $|+,\cdots,+\rangle$. Rather, we observe that $|\boldsymbol{\phi}(\boldsymbol{x})\rangle$ transitions from being z polarized in the spin glass phase to being almost fully polarized in the xy plane in the paramagnetic phase, encoding the information about the model's phase. Furthermore, the proportionality constant between $\overline{M_{nm}^2}$ and $1/N$ also shows a nontrivial dependence on g and h.

Phase transition at finite longitudinal fields.—Another nontrivial feature of the QSK model which can be studied thanks to our method is the presence of a phase transition at $h > 0$. It has been conjectured that the model's spin glass phase survives also for nonvanishing longitudinal fields h, suggesting the existence of a line of quantum phase transitions between the spin glass and paramagnetic phases that extends from the $g = g_C$, $h = 0$ critical point into the $h > 0$ plane (often referred to as the quantum de Almeida–Thouless line). This conjecture is however based on not yet conclusive investigations of the stability of replica symmetry breaking (RSB) at zero temperature [29,52].

Our variational analysis can tackle this issue without making assumptions about RSB. Indeed, we can extend our

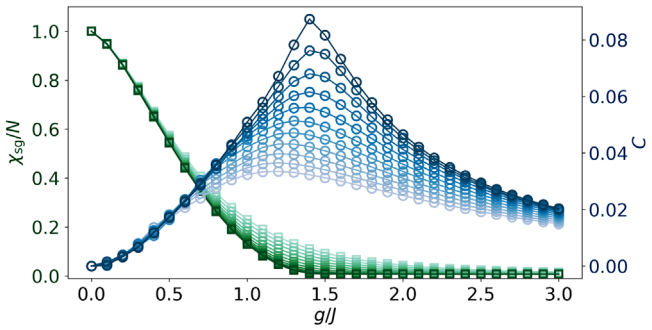

FIG. 5. Spin glass susceptibility per site χ_{sg}/N (green squares) and entropy coefficient C (blue circles) as functions of g for different values $h/J = 0, 0.1, \ldots, 1$ (dark to light) at $N = 150$. We observe that both functions develop a singularity typical of a phase transition only in the $h = 0$ limit.

analysis to variational ground states in the whole parameter space of the model, including $h > 0$. We observe that all indicators of a phase transition vanish as soon as $h > 0$.

More specifically, the spin glass susceptibility χ_{sg} becomes a smooth function of g whenever $h > 0$, no longer presenting the discontinuity in its derivative typical of a phase transition, even at large N. Similarly, the coefficient C characterizing the entropy behavior of the ground states clearly shows a singular behavior at $h = 0$ but not for finite h. These results are illustrated in Fig. 5. In conclusion, our analysis was not able to identify any sign of the conjectured phase transition in the $h > 0$ region. The discrepancy with previous results suggests this regime should be investigated further, especially in relation to RSB.

Conclusion.—We have shown that generalized atomic coherent states capture relevant properties of the ground states of the QSK model. The subset approximating the ground states contains a nontrivial entanglement structure, displaying a volume law, akin to the one of weighted graph states with random phase gates.

It is remarkable that the GCS resemble the quantum approximate optimization algorithm *Ansatz* [53,54] for the QSK model, with one Ising interaction layer sandwiched between two product operators. In our case, however, the parameters of these layers do not necessarily correspond to those of the Hamiltonian. Our results can thus inspire other quantum computing variational eigensolvers for QSK-like models, building on top of the states (3), something that deserves more detailed research.

T. G. acknowledges valuable discussions with Lorenzo Piroli and Nicola Pancotti. J. I. C. and T. G. are supported by the ERC Advanced Grant QUENOCOBA under the EU Horizon 2020 program (Grant Agreement No. 742102) and the German Research Foundation (DFG) under Germany's Excellence Strategy through Project No. EXC-2111-390814868 (MCQST). The project is part of the Munich Quantum Valley, which is supported by the Bavarian state government with funds from the Hightech Agenda Bayern Plus. P. M. S. has been financially supported by the Studienstiftung des Deutschen Volkes (German Scholarship Foundation). T. S. is supported by the NSFC (Grant No. 11974363). E. D. is supported by the ARO Grant No. W911NF-20-1-0163, AFOSR-MURI Photonic Quantum Matter Award No. FA95501610323, and the National Science Foundation through Grant No. NSF EAGER-QAC-QSA, Award No. 2222-206-2014111.

P. M. S. and T. G. contributed equally to this work.

*psch@pks.mpg.de
†tommaso.guaita@fu-berlin.de

[1] K. Binder and A. P. Young, Spin glasses: Experimental facts, theoretical concepts, and open questions, Rev. Mod. Phys. **58**, 801 (1986).
[2] H. Nishimori, *Statistical Physics of Spin Glasses and Information Processing: An Introduction* (Oxford University Press, Oxford, 2001).
[3] M. Baity Jesi, An introduction to spin glasses: History, simulations and phase transition, in *Spin Glasses: Criticality and Energy Landscapes* (Springer International Publishing, Cham, 2016), pp. 3–42.
[4] M. Mezard and A. Montanari, *Information, Physics, and Computation* (Oxford University Press, Inc., New York, 2009).
[5] S. Sachdev, Spin glasses enter the quantum regime, Phys. World **7**, 25 (1994).
[6] G. E. Santoro, R. Martoňák, E. Tosatti, and R. Car, Theory of quantum annealing of an Ising spin glass, Science **295**, 2427 (2002).
[7] T. Albash and D. A. Lidar, Adiabatic quantum computation, Rev. Mod. Phys. **90**, 015002 (2018).
[8] C. L. Baldwin and C. R. Laumann, Quantum algorithm for energy matching in hard optimization problems, Phys. Rev. B **97**, 224201 (2018).
[9] V. Bapst, L. Foini, F. Krzakala, G. Semerjian, and F. Zamponi, The quantum adiabatic algorithm applied to random optimization problems: The quantum spin glass perspective, Phys. Rep. **523**, 127 (2013).
[10] E. Farhi, J. Goldstone, S. Gutmann, and L. Zhou, The quantum approximate optimization algorithm and the Sherrington-Kirkpatrick model at infinite size, Quantum **6**, 759 (2022).
[11] D. Sherrington and S. Kirkpatrick, Solvable Model of a Spin-Glass, Phys. Rev. Lett. **35**, 1792 (1975).
[12] H. Ishii and T. Yamamoto, Effect of a transverse field on the spin glass freezing in the Sherrington-Kirkpatrick model, J. Phys. C **18**, 6225 (1985).
[13] K. Usadel, Spin glass transition in an Ising spin system with transverse field, Solid State Commun. **58**, 629 (1986).
[14] D. Thirumalai, Q. Li, and T. R. Kirkpatrick, Infinite-range Ising spin glass in a transverse field, J. Phys. A **22**, 3339 (1989).
[15] T. Yamamoto and H. Ishii, A perturbation expansion for the Sherrington-Kirkpatrick model with a transverse field, J. Phys. C **20**, 6053 (1987).

[16] K. Takahashi, Quantum fluctuations in the transverse Ising spin glass model: A field theory of random quantum spin systems, Phys. Rev. B **76**, 184422 (2007).

[17] Y. Y. Goldschmidt and P.-Y. Lai, Ising Spin Glass in a Transverse Field: Replica-Symmetry-Breaking Solution, Phys. Rev. Lett. **64**, 2467 (1990).

[18] J. Miller and D. A. Huse, Zero-Temperature Critical Behavior of the Infinite-Range Quantum Ising Spin Glass, Phys. Rev. Lett. **70**, 3147 (1993).

[19] J. V. Alvarez and F. Ritort, Quantum Monte Carlo study of the infinite-range Ising spin glass in a transverse field, J. Phys. A **29**, 7355 (1996).

[20] P.-Y. Lai and Y. Y. Goldschmidt, Monte Carlo studies of the Ising spin-glass in a transverse field, Europhys. Lett. **13**, 289 (1990).

[21] P. Ray, B. K. Chakrabarti, and A. Chakrabarti, Sherrington-Kirkpatrick model in a transverse field: Absence of replica symmetry breaking due to quantum fluctuations, Phys. Rev. B **39**, 11828 (1989).

[22] B. K. Chakrabarti, A. Dutta, and P. Sen, *Quantum Ising Phases and Transitions in Transverse Ising Models* (Springer, New York, 1996), Vol. 41.

[23] A. Das and B. K. Chakrabarti, Reaching the ground state of a quantum spin glass using a zero-temperature quantum Monte Carlo method, Phys. Rev. E **78**, 061121 (2008).

[24] S. Mukherjee, A. Rajak, and B. K. Chakrabarti, Classical-to-quantum crossover in the critical behavior of the transverse-field Sherrington-Kirkpatrick spin glass model, Phys. Rev. E **92**, 042107 (2015).

[25] K. Takahashi and Y. Matsuda, Energy-gap analysis of quantum spin-glass transitions at zero temperature, J. Phys. Conf. Ser. **233**, 012008 (2010).

[26] Y. W. Koh, Effects of low-lying excitations on ground-state energy and energy gap of the Sherrington-Kirkpatrick model in a transverse field, Phys. Rev. B **93**, 134202 (2016).

[27] S. Mukherjee, S. Nag, and A. Garg, Many-body localization-delocalization transition in the quantum Sherrington-Kirkpatrick model, Phys. Rev. B **97**, 144202 (2018).

[28] S. Mukherjee, A. Rajak, and B. K. Chakrabarti, Possible ergodic-nonergodic regions in the quantum Sherrington-Kirkpatrick spin glass model and quantum annealing, Phys. Rev. E **97**, 022146 (2018).

[29] A. P. Young, Stability of the quantum Sherrington-Kirkpatrick spin glass model, Phys. Rev. E **96**, 032112 (2017).

[30] S. Pappalardi, A. Polkovnikov, and A. Silva, Quantum echo dynamics in the Sherrington-Kirkpatrick model, SciPost Phys. **9**, 21 (2020).

[31] G. Parisi, A sequence of approximated solutions to the S-K model for spin glasses, J. Phys. A **13**, L115 (1980).

[32] D. Panchenko, The Sherrington-Kirkpatrick model: An overview, J. Stat. Phys. **149**, 362 (2012).

[33] L. Arrachea and M. J. Rozenberg, Dynamical Response of Quantum Spin-Glass Models at $T = 0$, Phys. Rev. Lett. **86**, 5172 (2001).

[34] M. J. Rozenberg and D. R. Grempel, Dynamics of the Infinite-Range Ising Spin-Glass Model in a Transverse Field, Phys. Rev. Lett. **81**, 2550 (1998).

[35] Note that in part of the literature a different convention is chosen when defining the Hamiltonian (1), omitting the factor $1/2$ in the Ising coupling term. This difference has to be taken into account when comparing the critical transverse fields obtained by different authors.

[36] T. Guaita, L. Hackl, T. Shi, E. Demler, and J. I. Cirac, Generalization of group-theoretic coherent states for variational calculations, Phys. Rev. Res. **3**, 023090 (2021).

[37] L. Hartmann, J. Calsamiglia, W. Dür, and H. J. Briegel, Weighted graph states and applications to spin chains, lattices and gases, J. Phys. B **40**, S1 (2007).

[38] S. Anders, M. B. Plenio, W. Dür, F. Verstraete, and H.-J. Briegel, Ground-State Approximation for Strongly Interacting Spin Systems in Arbitrary Spatial Dimension, Phys. Rev. Lett. **97**, 107206 (2006).

[39] S. Anders, H. J. Briegel, and W. Dür, A variational method based on weighted graph states, New J. Phys. **9**, 361 (2007).

[40] F. T. Arecchi, E. Courtens, R. Gilmore, and H. Thomas, Atomic coherent states in quantum optics, Phys. Rev. A **6**, 2211 (1972).

[41] M. Foss-Feig, K. R. A. Hazzard, J. J. Bollinger, and A. M. Rey, Nonequilibrium dynamics of arbitrary-range Ising models with decoherence: An exact analytic solution, Phys. Rev. A **87**, 042101 (2013).

[42] See Supplemental Material at http://link.aps.org/supplemental/10.1103/PhysRevLett.129.220401 for more details.

[43] L. Hackl, T. Guaita, T. Shi, J. Haegeman, E. Demler, and J. I. Cirac, Geometry of variational methods: Dynamics of closed quantum systems, SciPost Phys. **9**, 48 (2020).

[44] C. Lanczos, An iteration method for the solution of the eigenvalue problem of linear differential and integral operators, J. Res. Natl. Bur. Stand. **45**, 255 (1950).

[45] The fact that the point of maximal error moves with N to larger g implies that for some g's in the interval $[1.0J, 1.5J]$ the error increases with N at fixed g. We expect this increase to be temporary and to saturate somewhere below the maximal error value, which we observe to decrease with N.

[46] See the left-hand panel of Fig. 2 for what concerns the spin glass susceptibility and the Supplemental Material for the σ^x magnetization [42].

[47] P. Sen, P. Ray, and B. K. Chakrabarti, Quantum critical behavior of the infinite-range transverse Ising spin glass: An exact numerical diagonalization study, arXiv:cond-mat/9705297.

[48] H. Leschke, C. Manai, R. Ruder, and S. Warzel, Existence of Replica-Symmetry Breaking in Quantum Glasses, Phys. Rev. Lett. **127**, 207204 (2021).

[49] A. Pal and D. A. Huse, Many-body localization phase transition, Phys. Rev. B **82**, 174411 (2010).

[50] M. Koashi and A. Winter, Monogamy of quantum entanglement and other correlations, Phys. Rev. A **69**, 022309 (2004).

[51] B. M. Terhal, Is entanglement monogamous?, IBM J. Res. Dev. **48**, 71 (2004).

[52] C. Manai and S. Warzel, The de Almeida–Thouless line in hierarchical quantum spin glasses, J. Stat. Phys. **186**, 14 (2022).

[53] E. Farhi, J. Goldstone, and S. Gutmann, A quantum approximate optimization algorithm, arXiv:1411.4028.

[54] M. Cerezo, A. Arrasmith, R. Babbush, S. C. Benjamin, S. Endo, K. Fujii, J. R. McClean, K. Mitarai, X. Yuan, L. Cincio, and P. J. Coles, Variational quantum algorithms, Nat. Rev. Phys. **3**, 625 (2021).